

Supplementary Information

Predicting the Mechanical Properties of Organic Semiconductors Using Coarse-Grained Molecular Dynamics Simulations

Samuel E. Root, Suchol Savagatrup, Christopher J. Pais, Gaurav Arya,* and Darren J. Lipomi*

Department of NanoEngineering, University of California, San Diego
9500 Gilman Drive, Mail Code 0448, La Jolla, CA 92093-0448

S1. Complete Description of Model Parameters

S1.1 Three-Site Model

The parameters for the three-site model were derived using the iterative Boltzmann inversion technique described in detail in reference 1. We note that the intramolecular potential parameters used here are from reference 5, they are slightly modified from the original publication to better represent the rigidity of the thiophene rings (intermonomer torsion) as described in detail in reference 2. In addition to this, the intermolecular parameters were fit to a Lennard-Jones 9-6 potential instead of using the tabulated potential described in reference 1.

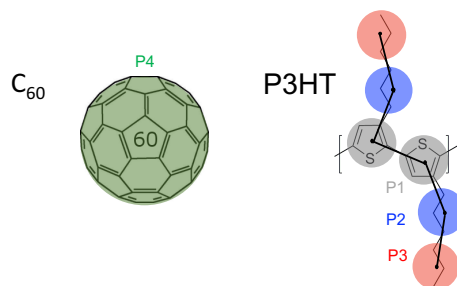


Figure S1. Coarse-grained mapping for the three-site model for P3HT:C₆₀.

Table S1. Intermolecular potentials and parameters for three-site model, coarse-grained bead definitions are given in Figure S1.

Intermolecular Potentials	Pairwise Interaction	σ [Å]	ϵ [kcal mol ⁻¹]	Δ [Å]	Cutoff [Å]
$E(r) = 4\epsilon \left[\left(\frac{\sigma}{r} \right)^9 - \left(\frac{\sigma}{r} \right)^6 \right]$	P1-P1	4.6	0.35	-	15
	P1-P2	4.3	1.45	-	15
	P1-P3	4.71	0.51	-	15
	P2-P2	4.7	1.57	-	15
	P2-P3	4.8	0.9	-	15
	P3-P3	4.89	0.55	-	15
$E(r) = 4\epsilon \left[\left(\frac{\sigma}{r-\Delta} \right)^{12} - \left(\frac{\sigma}{r-\Delta} \right)^6 \right]$	P4-P1	5.3	1.37	1.4	16.6
	P4-P2	5.3	2.35	1.7	16.4
	P4-P3	5.3	1.32	1.8	16.2
	P4-P4	3.841	5.55	5.76	12.234

Table S2. Intramolecular potentials and parameters used for the three-site model, coarse-grained bead definitions are given in Figure S1.

Intramolecular Potentials	Bonded								
	Interaction	l_0 [Å]	c_2 [kcal/mol/Å ²]	c_3 [kcal/mol/Å ³]	c_4 [kcal/mol/Å ⁴]	c_5 [kcal/mol/Å ⁵]	c_6 [kcal/mol/Å ⁶]	c_7 [kcal/mol/Å ⁷]	c_8 [kcal/mol/Å ⁸]
$E_{bond}(l) = \sum_{i=2}^n c_i (l - l_0)^i$	P1-P1	3.862	74.8542	--	--	--	--	--	--
	P1-P2	4.095	58.818	175.482	146.518	--	--	--	--
	P2-P3	3.5786	20.8811	-12.6477	-161.456	-50.2732	634.945	941.494	392.644

Angular Interactions	θ_0	c_2	c_3	c_4	
	[deg.]	[kcal/mol/rad ²]	[kcal/mol/rad ³]	[kcal/mol/rad ⁴]	
$E_{angle}(\theta) = \sum_{i=0}^n c_i (\theta - \theta_0)^i$	P1-P1-P1	163.161	11.256	49.983	109.974
	P1-P2-P3	157.196	9.415	10.9533	4.66974
	P1-P1-P2	123.473	--	-14.3575	61.8653
	P2-P1-P1	78.904	--	-2.27575	35.9306

Dihedral Interactions	c_1	c_2	c_3	c_4	c_5	
	[kcal/mol]	[kcal/mol]	[kcal/mol]	[kcal/mol]	[kcal/mol]	
$E_{dihed}(\phi) = \sum_{i=0}^n c_i \cos^i(\phi)$	P1-P1-P1-P1	1.00335	-0.098468	-0.145065	-0.596209	-0.22064
	P2-P1-P1-P2	1.43524	0.323256	-1.31207	0.357231	0.557297
	P1-P1-P2-P3	0.217212	-0.603055	0.194054	0.349013	-0.004806
	P3-P2-P1-P1	-0.017475	0.018428	0.4546	0.116077	-0.075817

Improper Interactions	φ_0	c_2
	[deg.]	[kcal/mol/rad ²]
P1-P2-P1-P1	0.00	45.3281

S1.1 One-Site Model

The parameters for the one-site model were taken directly from reference 3. We note that we also implemented the stylistically similar potential described in reference 4, and observed similar results.

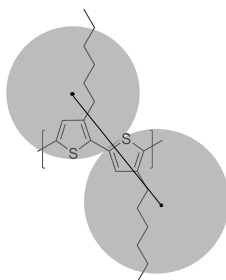


Figure S2. Coarse-grained mapping for the one-site model for P3HT.

Table S3. Intra/intermolecular potentials and parameters used for the one-site model representing P3HT, coarse-grained bead definitions are given in Figure S2.

	Intra/intermolecular Potential	Parameters
Bond	$E_{bond}(l) = \frac{k_b}{2}(l - l_0)^2$	$k_b = 216.19 \text{ kcal mol}^{-1} \text{ \AA}^{-2}$ $l_0 = 3.82 \text{ \AA}$
Angle	$E_{angle}(\theta) = \frac{k_\theta}{2}(\theta - \theta_0)^2$	$k_\theta = 130.25 \text{ kcal mol}^{-1} \text{ rad}^{-2}$ $\theta_0 = 2.65 \text{ rad}$
Dihedral	$E_{dihed}(\phi) = \frac{V_1}{2}(1 + \cos\phi) + \frac{V_2}{2}(1 - \cos 2\phi) + \frac{V_3}{2}(1 + \cos 3\phi)$	$V_1 = 0.56 \text{ kcal mol}^{-1}$ $V_2 = -1.08 \text{ kcal mol}^{-1}$ $V_3 = 0.28 \text{ kcal mol}^{-1}$
Van Der Waals	$E_{VDW}(r) = 4\epsilon \left[\left(\frac{\sigma}{r}\right)^{12} - \left(\frac{\sigma}{r}\right)^6 \right]$	$\epsilon = 0.26 \text{ kcal mol}^{-1}$ $\sigma = 4.95 \text{ \AA}$

S2. Analysis of Entanglements using Z1 Code

To compare the density of entanglements in the pure and composite systems we applied the Z1 algorithm developed by Kröger et al. (references 6-9) to compute the primitive paths of the polymer chains, shown in Figure S3. The physical quantities obtained from this analysis are shown in Table S4. Briefly, the quantity $\langle Z \rangle$ represents the average number of interior kinks per chain, $\langle L_{pp}^2 \rangle$ is average squared contour length between interior kinks and N_e is entanglement length which varies depending on which estimator is used (modified S-kink vs. modified S-coil), for a detailed explanation of these estimators see ref. 7.

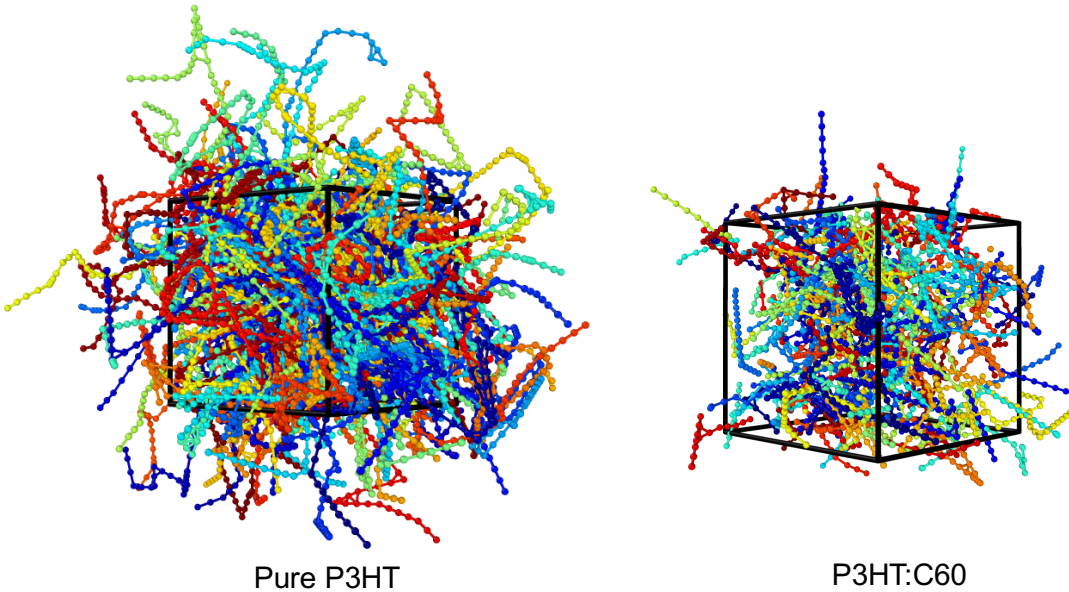


Figure S3. Plots showing the primitive paths obtained using the Z1 algorithm

Table S4. Physical parameters obtained from the Z1 primitive path analysis.

	$\langle Z \rangle$	$\langle L_{pp}^2 \rangle$ [\AA^2]	Ne modified S-kink	Ne modified S-coil
Pure P3HT	7.0467	352.2057	21.2867	41.3626
P3HT:C60	2.4	140.0633	62.5	106.8907

S3. Extension of Three-Site Model Using Original Interaction Parameters

In an attempt to describe a range of P3AT's with different alkyl side-chain lengths (hexyl, nonyl, and dodecyl), we modified the original three-site model for P3HT to include extra coarse-grained beads on the side chain as shown in Figure S3a. Our simulations for the stress-strain response of these materials (Figure S3b) showed that the tensile modulus increased with side-chain length, which is contrary to experimental results. Upon closer inspection of the interaction parameters from the original model (Table S1) we noted that the interactions between the side chains were stronger than the interactions between the thiophene rings in the backbone. We attribute this to the simultaneous nature in which these parameters were optimized, leading to a model that worked correctly for P3HT, but that was not transferable across a range of chemical structures.

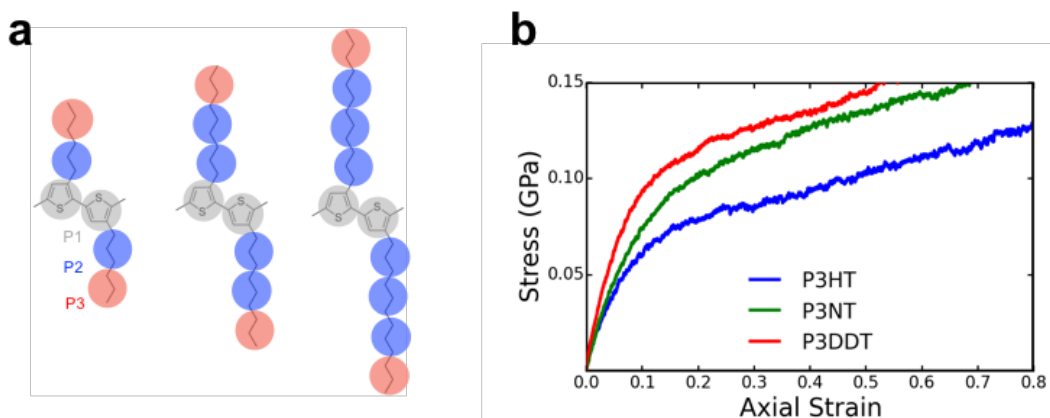


Figure S4. Original extension made to the three-site model to describe P3AT's (a) extension of alkyl side-chain using coarse-grained bead definitions from Figure S1 and Table S1, S2. (b) Initial results showing increasing tensile modulus with side-chain length (in contradiction with experimental results, indicating limited transferability of the model.)

- (1) Huang, D. M.; Faller, R.; Do, K.; Moule, A. J. Coarse-Grained Computer Simulations of Polymer / Fullerene Bulk Heterojunctions for Organic Photovoltaic Applications. *J. Chem. Theory Comput.* **2010**, *6*, 526-537.
- (2) Schwarz, K. N.; Kee, T. W.; Huang, D. M. Coarse-Grained Simulations of the Solution Phase Self-Assembly of poly(3-Hexylthiophene) Nanostructures. *Nanoscale* **2013**, *5* (5), 2017-2027.
- (3) Lee, C.-K.; Pao, C.-W.; Chu, C.-W. Multiscale Molecular Simulations of the Nanoscale Morphologies of P3HT:PCBM Blends for Bulk Heterojunction Organic Photovoltaics *Energy Environ. Sci.* **2011**, *4*, 4124-4132.
- (4) Lee, C. K.; Pao, C. W. Nanomorphology Evolution of P3HT:PCBM Blends during Solution Processing from Coarse-Grained Molecular Simulations *J. Phys. Chem. C* **2014**, *118*, 11224-11233.
- (5) Jones, M. L.; Huang D.M.; Chakrabarti, B.; Groves, C. Relating Molecular Morphology to Charge Mobility in Semicrystalline Conjugated Polymers. *J. Phys. Chem C.* **2016**, *8*, 4240-4250.
- (6) Kröger, M. Shortest Multiple Disconnected Path for the Analysis of Entanglements in Two- and Three-Dimensional Polymeric Systems. *Comput. Phys. Commun.* **2005**, *168*, 209–232.
- (7) Hoy, R. S.; Foteinopoulou, K.; Kröger, M. Topological Analysis of Polymeric Melts: Chain-Length Effects and Fast-Converging Estimators for Entanglement Length. *Phys. Rev. E - Stat. Nonlinear, Soft Matter Phys.* **2009**, *80*, 14–16.
- (8) Shanbhag, S.; Kröger, M. Primitive Path Networks Generated by Annealing and Geometrical Methods: Insights into Differences. *Macromolecules* **2007**, *40*, 2897–2903.